# Brain conditioning is instrumental for successful microglia reconstitution following hematopoietic stem cell transplantation

Alessia Capotondo[a,b], Rita Milazzo[a,b], Letterio Salvatore Politi[c,d], Angelo Quattrini[e], Alessio Palini[f], Tiziana Plati[a], Stefania Merella[a], Alessandro Nonis[g], Clelia di Serio[g], Eugenio Montini[a], Luigi Naldini[a,b], and Alessandra Biffi[a,1]

[a]San Raffaele Telethon Institute for Gene Therapy, Division of Regenerative Medicine, Stem Cells and Gene Therapy, [b]Vita-Salute San Raffaele University, [c]Imaging Core, [d]Neuroradiology Unit, Head and Neck Department, [e]Division of Neuroscience, [f]Flow Cytometry Resource Analytical Cytology Technical Applications Laboratory, and [g]Center of Biostatistics, Vita-Salute San Raffaele University, San Raffaele Scientific Institute, 20132 Milan, Italy

Edited by Irving L. Weissman, Stanford University, Palo Alto, CA, and approved July 16, 2012 (received for review April 19, 2012)

**The recent hypothesis that postnatal microglia are maintained independently of circulating monocytes by local precursors that colonize the brain before birth has relevant implications for the treatment of various neurological diseases, including lysosomal storage disorders (LSDs), for which hematopoietic cell transplantation (HCT) is applied to repopulate the recipient myeloid compartment, including microglia, with cells expressing the defective functional hydrolase. By studying wild-type and LSD mice at diverse time-points after HCT, we showed the occurrence of a short-term wave of brain infiltration by a fraction of the transplanted hematopoietic progenitors, independently from the administration of a preparatory regimen and from the presence of a disease state in the brain. However, only the use of a conditioning regimen capable of ablating functionally defined brain-resident myeloid precursors allowed turnover of microglia with the donor, mediated by local proliferation of early immigrants rather than entrance of mature cells from the circulation.**

Microglia are the resident immune cells of the central nervous system (CNS) and belong to the mononuclear phagocyte lineage (1). Currently, they are believed to originate from ontogenically distinct primitive myeloid progenitors that during the embryonic stage invade the developing brain, where they transform into the resting ramified microglia of the mature CNS (2). Different hypotheses exist about how microglia are maintained in adulthood: it was proposed that microglia only self-renew themselves via in situ proliferation from resident progenitors, but also that their pool is replenished from circulating progenitors. Several in vitro (3, 4) and in vivo (5–9) studies addressed this issue, and most recent literature suggested that postnatal microglia are maintained independently of circulating monocytes by local radio-resistant precursors that colonize the brain before birth (2). Such evidence has relevant implications for the treatment of various neurological disorders, including lysosomal storage disorders (LSDs).

Over the past three decades, ∼1,000 hematopoietic cell transplantations (HCTs) have been performed worldwide for patients with different LSDs in the attempt to slow the course of the disease, prevent symptoms onset, and improve pathological findings (10–12). The aim of HCT in these disorders is to repopulate the recipient myeloid compartment, including microglia, with cells expressing the hydrolase that is defective in the recipient (13). Because macrophage and microglia represent the major effectors of the catabolism of the storage material throughout the tissues, their replacement by normal cells restores a critical scavenging function. Moreover, these cells can secrete a portion of their lysosomal enzymes, which can be taken up by neighboring cells, which are thus corrected in their metabolic defect (13). From the impressive results obtained in Hurler syndrome (11), it was expected that most LSDs could be alleviated by HCT. However, HCT proved to be ineffective in LSD patients with severe CNS involvement and, in particular, in those having overt neurological symptoms and/or aggressive early onset forms (10). The main reason for HCT failure in these patients is likely the slow pace of replacement, if any, of resident CNS microglia by the transplanted hematopoietic cell progeny, compared with the rapid progression of the primary neurological disease. Indeed, although the reconstitution of visceral organ macrophages by donor-derived cells has been clearly established after HCT, substantial debate (8, 9) and poor knowledge exist on the actual occurrence, modalities, and timing of CNS microglia replacement by the progeny of the transplanted hematopoietic cells.

Here, we used a multidisciplinary approach to study the brain myeloid compartment of wild-type (WT) and LSD mice at diverse time-points after HCT and provide evidence of extensive bona fide microglia reconstitution only upon (*i*) migration and engraftment in the brain of donor cells capable of intraparenchymal proliferation and (*ii*) pharmacological ablation of an endogenous proliferating myeloid cell pool, which could likely contribute to microglia maintenance in physiological conditions.

## Results

**Donor Myeloid Infiltration Occurs in the Brain of Naïve Mice.** We used a multidisciplinary approach based on magnetic resonance imaging (MRI), flow cytometry, and immunohistology to monitor the fate of hematopoietic stem and progenitor cells (HSPCs), retrieved by lineage negative ($Lin^-$) selection from the murine bone marrow (BM), upon transplantation into naïve congenic recipients. Superparamagnetic iron oxide (SPIO) particles were used for rendering HSPCs detectable by MRI in short-term studies (14, 15), whereas GFP-encoding lentiviral vectors (LVs) were used to track genetically marked cells long-term (Fig. S1). Double-labeled (DL)-HSPCs were i.v. transplanted into naïve, 2-mo-old WT or LSD mice [we used the $As2^{-/-}$ model of metachromatic leukodystrophy (MLD), a prototypical LSD with CNS involvement] (Fig. S2*A*). Short term after HCT, upon mice perfusion, MRI demonstrated multiple hypointense spots within the brain of the tested animals (Fig. 1 *A*, *C*, and *F*). Interestingly, the signal was detected only in mice transplanted with c-$Kit^+$ $Sca1^+Lin^-$ cells (KSL; enriched in stem cell activity) and not in animals receiving the not c-$Kit^+Sca1^+$ (not KS) $Lin^-$ counterpart (Fig. 1*C* and Fig. S1 *E–G*). Prussian blue staining, GFP immunofluorescence, and electron microscopy showed iron-containing, $GFP^+$ cells in areas consistent to those where MRI detected the hypointense spots (Fig. 1 *B*, *D*, and *E*). The number of spots detected in WT and MLD mice was similar (Fig. 1 *F* and *G*), whereas a notable difference in the location of the signal in the two groups was observed (Fig. 1 *F* and *H*), with abundant signal in the corpus callosum of MLD animals, where a delay in myelination is present (16).

Author contributions: A.B. and A.C. designed research; A.C., R.M., L.S.P., A.Q., A.P., T.P., S.M., and A.N. performed research; A.C., L.S.P., C.d.S., E.M., L.N., and A.B. analyzed data; and A.B. wrote the paper.

The authors declare no conflict of interest.

This article is a PNAS Direct Submission.

[1]To whom correspondence should be addressed. E-mail: a.biffi@hsr.it.

This article contains supporting information online at www.pnas.org/lookup/suppl/doi:10.1073/pnas.1205858109/-/DCSupplemental.

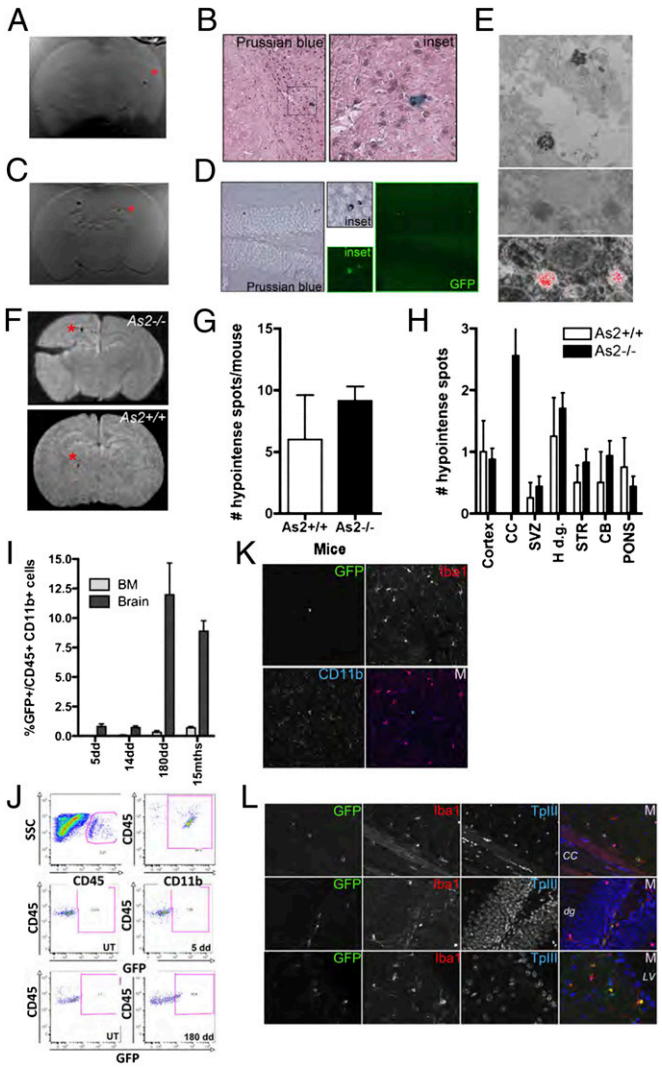


**Fig. 1.** Infiltration of DL-HSPCs in the brain of naïve mice. (*A* and *C*) Representative ex vivo MRI of the brain of As2$^{-/-}$ mice transplanted with DL-HSPCs (DL-HSPCs→As2$^{-/-}$) (*A*) or KSL cells (*C*) 5 d after HCT (T2* MR sequences by a 1.5 T human scanner). Hypointense spots within the brain are detected. (*B*) Iron-containing, Prussian blue$^{+}$ cells on brain sections from the As2$^{-/-}$ mouse shown in (*A*) [see (*)]. (*D*) Prussian blue staining (*Left*) and GFP immunofluorescence (*Right*) on brain sections from the As2$^{-/-}$ mouse shown in *C*. Cells positive for both signals [see (*)] are present. (*E*) EM showing electron-dense lysosomes (*Top* and *Middle*) corresponding to intraphagosomal iron on a brain section (MRI-proven site of migration) from a DL-HSPCs→As2$^{-/-}$ mouse, analyzed short term after HCT. The *Middle* and *Bottom* panels show colocalization of the intracellular iron particles (*Upper*) with positive signal on the corresponding iron map (red color; *Lower*) obtained at 250 eV by ESI. (*F*) Representative brain ex vivo MRI of the brain of DL-HSPCs→As2$^{-/-}$ (*Upper*) and As2$^{+/+}$ (*Lower*) mice examined 5 d after HCT (T2* MR sequences by a 3 T human scanner). A similar number of hypointense spots (see red *) is detected, but only in the As2$^{-/-}$ mouse the spots are located at the corpus callosum. (*G*) Quantification of the MRI hypointense spot number (#) in the brain of As2$^{+/+}$ and As2$^{-/-}$ mice. Mean and SEM are shown; $n = 26$ for As2$^{+/+}$ and $n = 37$ for As2$^{-/-}$ mice. (*H*) Distribution of the hypointense spots in the indicated brain areas as in *G*; CB, cerebellum; Cortex, cortical gray matter; H.d.g., hippocampal dentate gyrus; STR, striatum; SVZ, subventricular zone. (*I*) GFP$^{+}$ cell frequency within CD45$^{+}$CD11b$^{+}$ cells from the BM and brain of GFP$^{+}$HSPC→mice, analyzed at 5, 14, and 180 d (dd) and 15 mo (mths) after HCT (pool of As2$^{+/+}$ and As2$^{-/-}$ mice, $n = 10$ per time-point). (*J*) CD45$^{+}$CD11b$^{+}$ cells (*Top*) and GFP$^{+}$ cells within CD45$^{+}$CD11b$^{+}$ cells in brains analyzed short- (5dd; *Middle*) or long-term (180dd; *Bottom*) after HCT (*Right*). UT, untransplanted mouse (*Left*). (*K* and *L*) Confocal images from brain sections of DL-HSPC As2$^{-/-}$ mice short- (*K*) and long-term (*L*) after HCT. Expression of GFP, Iba-1 (red), and CD11b (blue) is shown. ToPROIII (TpIII) for nuclei. M, merge; cc, corpus callosum; d.g., dentate gyrus; LV, lateral ventricle.

Analysis of GFP expression within the brain myeloid compartment of the transplanted mice by flow-cytometry confirmed the presence of donor cells short term after HCT (Fig. 1 *I* and *J*). Long-term analysis up to 15 mo after HCT revealed persistence and limited expansion of these cells, despite their virtual absence from the BM (Fig. 1 *I* and *J*). Both at short- and long-term after HCT, the GFP$^{+}$ cells were round and small hematopoietic lineage cells and expressed at low levels the myeloid markers Iba1 and CD11b (Fig. 1 *K* and *L*) without evidence of mature microglia reconstitution even in the long term (Fig. 1*L*). The cells were mostly found in areas of short-term homing, being more abundant in adult neurogenic areas and in the corpus callosum of MLD mice (Fig. 1*L*).

To assess the therapeutic potential of the cells engrafted in the brain of naïve mice, we tested the activity of arylsulfatase A (ARSA; the defective enzyme in MLD) in the brain of As2$^{-/-}$ mice transplanted with WT HSPCs long term after HCT (7). However, no significant increase in ARSA activity could be detected at comparison with untreated MLD littermates ($0.9 \pm 0.04$ fold vs. the untreated As2$^{-/-}$ mice activity level, $n \geq 3$).

**Macrophage/Microglia Replacement in the Brain of Preconditioned Mice.** We then assessed whether the administration of a preparative regimen before HCT, allowing for engraftment of the donor cells into hematopoietic organs, could lead to reconstitution of microglia. We compared widely used regimens differing in their capability to cross the blood–brain barrier (BBB) and cause CNS toxicity (7, 17). In particular, treosulfan (TREO) is the only regimen, among the tested ones, unable to cross the BBB. Pretreated adult WT or MLD mice were transplanted with labeled congenic HSPCs and analyzed as described above (Fig. S2*B*).

Labeled cells were detected in the brain of transplanted mice by 5 d after HCT, with a similar frequency and location in all of the transplant groups (Fig. 2*A*). At longer time points, once sustained donor chimerism was established in the BM (Fig. S3), the frequency of GFP$^{+}$ cells within brain myeloid populations differed between the animals according to (*i*) the time at analysis, (*ii*) the regimen applied before HCT, and (*iii*) the CD45$^{+}$CD11b$^{+}$ subpopulation considered (18–20) (Fig. 2 *A*–*H*) (for details on cell populations, see Fig. S4). GFP$^{+}$CD45$^{+}$CD11b$^{+}$ cells were present at all of the time-points and with increasing frequency over time; however, fewer GFP$^{+}$ cells were found in TREO and irradiated (IRR) mice compared with busulfan-treated (BU) animals (Fig. 2 *A* and *B*). GFP$^{+}$ cells were abundant within meningeal, perivascular, and choroid plexus macrophages (CNS-ϕ) in all of the groups, and their frequency progressively matched the one observed in the BM/peripheral blood, suggesting that this population turns over with circulating cells (Fig. 2 *G* and *H* and Fig. S3). Fewer GFP$^{+}$ cells were present within bona fide parenchymal microglia (μ cells) (Fig. 2 *C* and *D*), but their frequency increased over time in BU and IRR animals; no GFP$^{+}$ μ cells were found in TREO animals up to the longest follow up (Fig. 2 *C* and *D*). The frequency of GFP$^{+}$ cells within the population defined as immature and transiently amplifying microglia cells (TAμ cells) (Fig. S4) was intermediate between the ones observed in the μ and CNS-ϕ populations at each time-point, with more GFP$^{+}$ cells in BU mice compared with the other groups (Fig. 2 *E* and *F*). Analysis of mice transplanted with GFP-LV–labeled KSL cells or not KS Lin$^{-}$ cells revealed that the KSL fraction is the only HSPC fraction associated to sustained GFP chimerism within brain myeloid cells long-term after transplant (Fig. S5).

GFP$^{+}$Iba1$^{+}$CD11b$^{+}$CD45$^{+/low}$MHC$^{-}$ ramified parenchymal cells, frequently grouped in clusters, were observed at increasing frequency over time in BU mice at confocal analysis (Fig. 3 and Fig. S6); their morphology resembled that of microglia at different stages of maturation (19) (Fig. 3 and Fig. S6). GFP$^{+}$ ramified cells were present also in IRR mice, but their appearance in the brain was delayed in time and their morphology less mature (Fig. 3 and Fig. S6). Almost no GFP$^{+}$Iba1$^{+}$CD11b$^{+}$CD45$^{+/low}$MHC$^{-}$ cells were found in TREO mice (Fig. S6). Conversely, in all of the groups, we identified GFP$^{+}$Iba1$^{+}$CD11b$^{+}$CD45$^{+}$MHC$^{+}$ nonramified cells located at the meninges, perivascular spaces, and plexi (Fig. 3 and Fig. S6).

NEUROSCIENCE

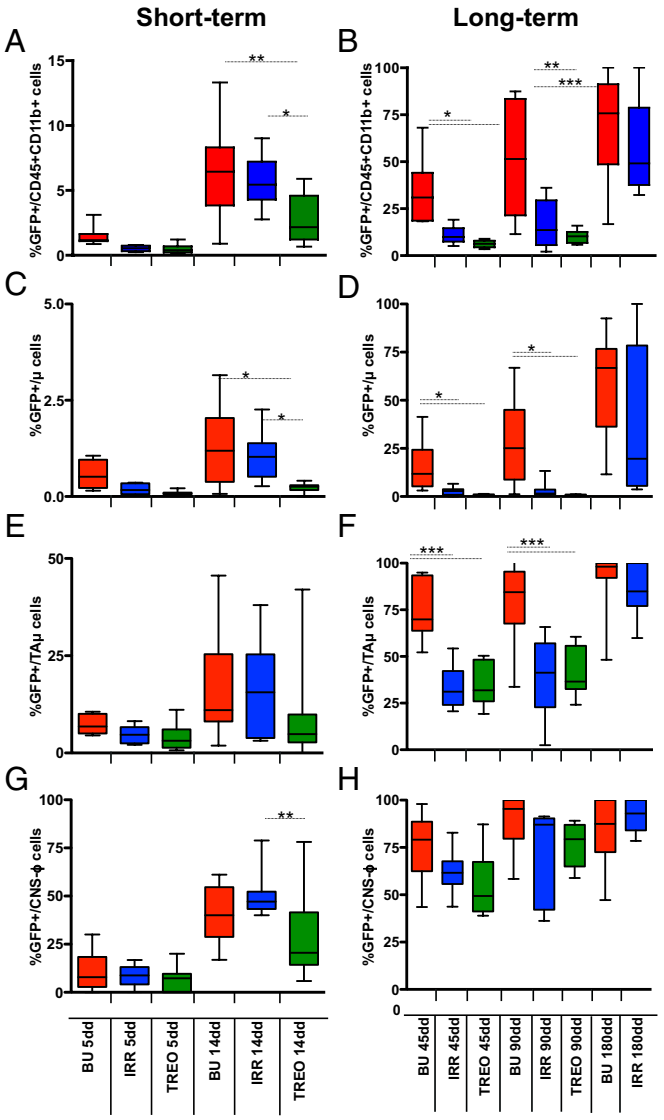


**Fig. 2.** Macrophage/microglia replacement in the brain of preconditioned mice. (*A–H*) Frequency (%) of GFP$^+$ cells within each indicated population, short and long term after HCT. $n \geq 10$ ($\geq$5 As2$^{+/+}$ and $\geq$5 As2$^{-/-}$) mice for each group at each time point. Mean and minimum/maximum values are shown; *$P < 0.05$, **$P < 0.01$, ***$P < 0.001$ at one-way ANOVA (with Bonferroni's post hoc test).

**Microglia Reconstitution by the Donor Is Associated to Depletion of the Endogenous Compartment.** We then assessed whether the conditioning could have had a direct effect on the endogenous brain myeloid compartment. Flow cytometry revealed a reduction in the frequency of myeloid cells in the brain of BU and IRR mice compared with untreated and TREO animals since 14–45 d after HCT (Fig. S7*A*). This reduction was associated to a progressive decline in μ cell relative frequency and to an increase in TAμ cell frequency in the same groups (Fig. 4 *A*, *B*, and *D*). At confocal analysis, endogenous microglia showed a senescent appearance with deramified morphology, and/or twisted and tortuous/stripped down processes (20), in BU animals evaluated 45 or more days after HCT (Fig. 4*C* and Fig. S7). Interestingly, the extent of μ cell depletion significantly correlated with the GFP chimerism within this same population (Fig. 4 *D* and *E*).

These long-term events were associated to the presence of a large fraction of apoptotic Annexin V$^+$ cells within CD45$^+$CD11b$^+$ cells (Fig. 4*F*) and of TUNEL$^+$ apoptotic Iba1$^+$ cells (Fig. 4*G*) in BU and, at a lower frequency, IRR mice 5–14 d after HCT. Apoptotic cells were negative for GFP and, therefore, bona fide host derived.

A microarray study performed on the whole brain of treated and control mice revealed the TNF-α mRNA to be increased in BU and, with a delayed kinetics, IRR animals short-term after treatment, which confirms the occurrence of apoptosis in these mice (Fig. S8) (21). Up-regulation of molecules involved in monocyte recruitment was transiently observed in IRR animals, consistent with what was described (Fig. S8) (9, 22).

**Depletion of Endogenous Proliferating Microglia and Proliferation of Donor Cells in the Brain Are Critical for Microglia Reconstitution.** To dissect the contribution of early brain immigrant vs. BM-derived circulating cells to microglia turnover with the donor, we set

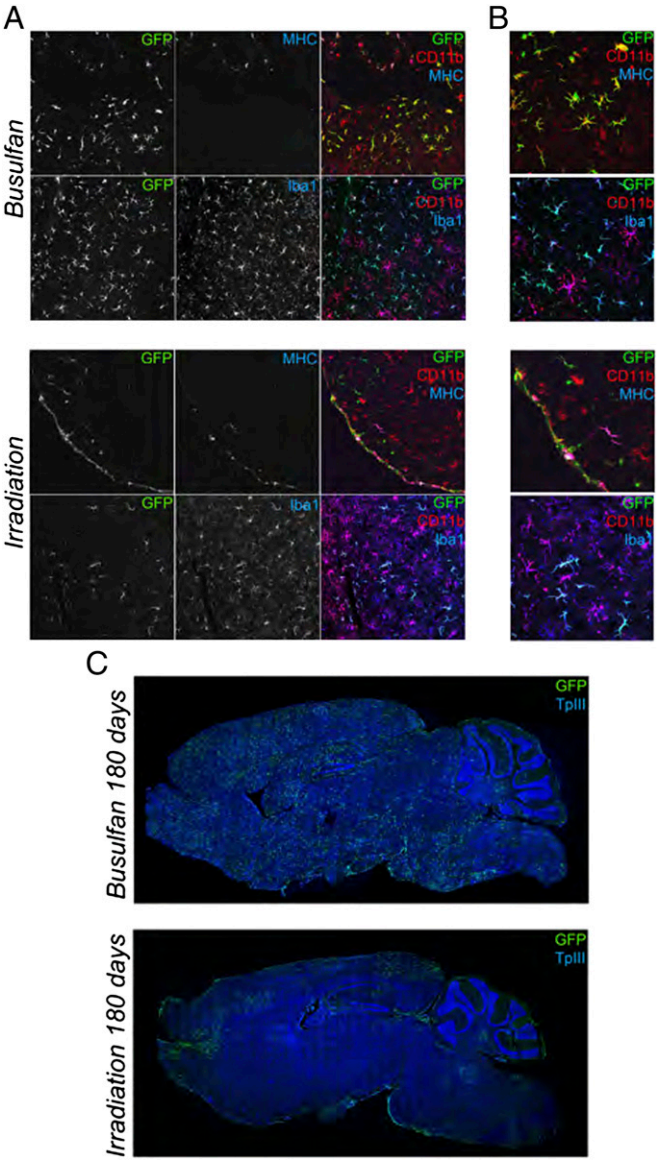


**Fig. 3.** Characterization of donor-derived cells in the brain of preconditioned mice. (*A* and *B*) Representative pictures showing IF staining for GFP, MHC class II, Iba-1, and CD11b on brain sections from GFP$^+$HSPCs→mice analyzed at 180 d after the HCT. TPIII: nuclei. Cells with small bodies and pronounced and abundant ramifications are present in BU-treated and irradiated mice at 180 d after HCT. (*C*) Distribution of GFP$^+$ cells in brain sections from representative BU-treated (*Upper*) and irradiated (*Lower*) As2$^{-/-}$ mice at 180 d after HCT. (Magnification: *A*, 20×; *B*, 50× compared with *A*.) Images were acquired at confocal microscope Radiance 2100 (Bio-Rad) (*A* and *B*), and Delta Vision Olympus Ix70 (*C*) and processed by the Soft Work 3.5.0; reconstructions were performed with Adobe Photoshop CS 8.0 software.

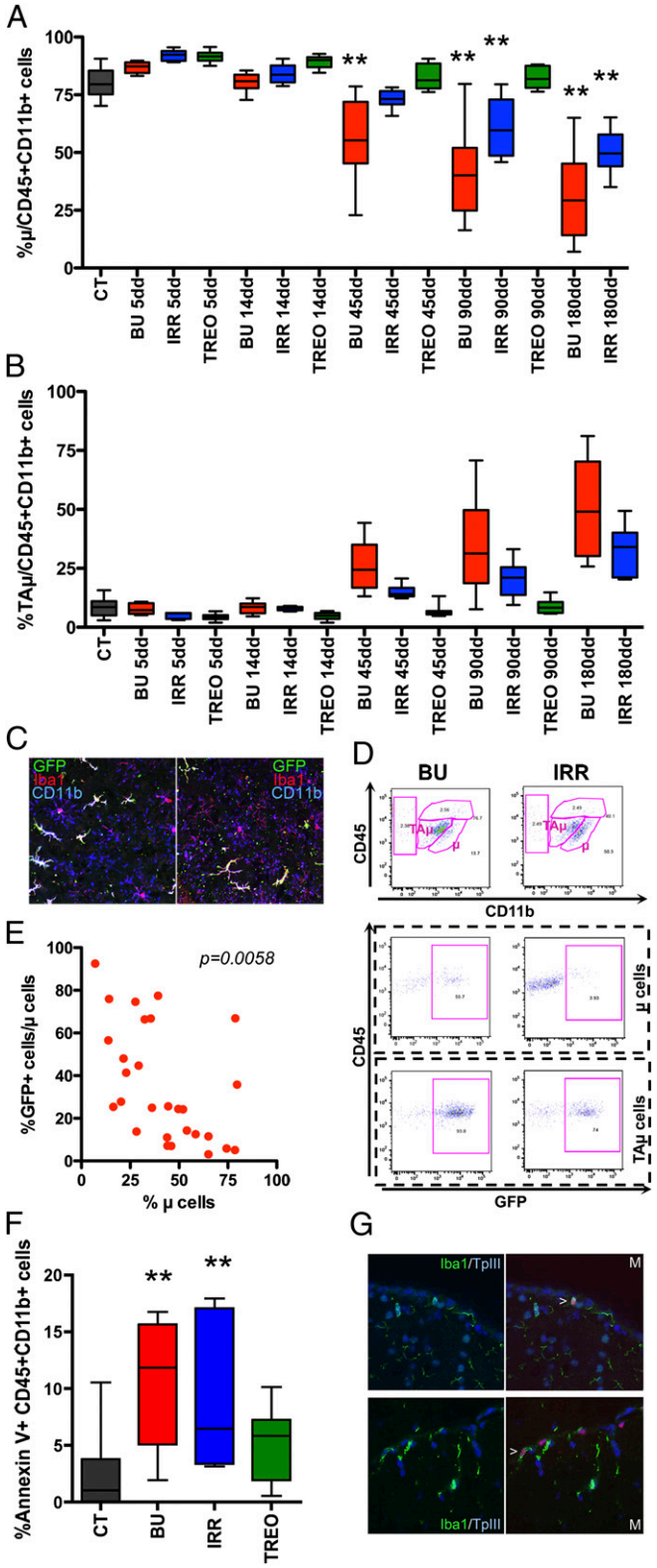


**Fig. 4.** Microglia reconstitution by donor cells associated to depletion of the endogenous microglia compartment. (*A* and *B*) Frequency of μ (*A*) and TAμ (*B*) cells of pretreated and transplanted mice at different times from HCT is shown. CT, untreated mice (no conditioning, no HCT). $n \geq 10$ ($\geq$5 As2$^{+/+}$ and $\geq$5 As2$^{-/-}$) mice per group for each time point. Mean and minimum/maximum values are shown; $^{*}P < 0.05$, $^{**}P < 0.01$ at one-way ANOVA (Dunnet's post hoc test). (*C*) Representative pictures showing abnormalities in the morphology of Iba-1$^{+}$CD11b$^{+}$GFP$^{-}$ host cells in BU-treated mice 3 mo after HCT. (*D*) Representative dot plots of the brain of BU-treated and irradiated mice 3 mo after HCT showing variations in the overall frequency and donor chimerism of μ and TAμ cells. (*E*) Correlation between the relative frequency (%) of μ cells and % GFP$^{+}$ cells within this population in the brain of BU-treated mice long term. The correlation *P* value is shown. (*F*) Frequency of Annexin V$^{+}$ cells within brain CD45$^{+}$CD11b$^{+}$ cells of conditioned mice 14 d after treatment. CT, untreated mice. $n \geq 10$ ($\geq$5 As2$^{+/+}$ and $\geq$5 As2$^{-/-}$) mice per group for each time point. Mean and minimum/maximum values are shown; $^{**}P < 0.01$ at one-way ANOVA (Dunnet's post hoc test). (*G*) Representative images showing TUNEL$^{+}$ (red) Iba-1$^{+}$ (green) cells on brain sections from mice at 14 d after BU (in blue nuclei by TPIII). M, merged panels. (Magnification: *C*, 80×; *G*, 100×.)

up a two-step transplant protocol in which busulfan and treosulfan were used to sequentially treat mice receiving differentially labeled cells (GFP$^{+}$ vs. ΔNGFR$^{+}$) (Fig. S2*C*). A transient BM engraftment of GFP$^{+}$ cells, transplanted as first, was observed after busulfan treatment and HCT (Fig. 5*A* and Fig. S9*B*). By 45 d after the second, treosulfan-mediated HCT, most of the GFP$^{+}$ cells disappeared from the recipients' BM and peripheral blood and sustained BM engraftment of the ΔNGFR$^{+}$ cells was observed (Fig. 5*A* and Fig. S9*B*). Consistently, liver CD45$^{+}$CD11b$^{+}$ cells were mostly ΔNGFR$^{+}$ (Fig. 5*A*). On the contrary, the brain myeloid pool was enriched in GFP$^{+}$ cells (Fig. 5*A*). The highest GFP/ΔNGFR ratio was observed in μ cells, whereas the lowest was present in CNS-ϕ (Fig. 5*A*). A progressive expansion of the donor-derived cells in the brain was observed between days 45 and 180 and it was mostly due to an increased frequency of transgene$^{+}$ μ cells; this expansion was mediated both by GFP$^{+}$ and ΔNGFR$^{+}$ cells (Fig. 5*A*). Confocal analysis demonstrated the presence of abundant GFP$^{+}$Iba1$^{+}$CD11b$^{+}$ ramified cells in brains analyzed at 45–180 d after the second HCT (Fig. 5 *B–D*). Also, ΔNGFR$^{+}$Iba1$^{+}$CD11b$^{+}$ were found, with a less mature morphology and at lower frequency (Fig. 5 *B–D*). A depletion of microglia, having a senescent appearance at confocal analysis, and expansion of TAμ cells were also observed (Fig. S9*D*).

To understand how, in the presence of a very low frequency of GFP$^{+}$ cells in peripheral blood, a sustained and dynamically expanding GFP chimerism could be obtained in the brain, we administered 5-ethynyl-2′-deoxiuridine (EdU) before mice killing and quantified proliferation of brain myeloid cells by cytofluorimetry. Interestingly, a larger fraction of proliferating cells was noticed in the transplanted animals compared with untreated age-matched controls (Fig. 5 *E* and *F*). The majority of these cells was of donor origin and composed by GFP$^{+}$ and ΔNGFR$^{+}$ elements in similar proportions (Fig. 5*G*). The proliferating cells were mostly contained in the μ population (Fig. 5*H*). Confocal analysis confirmed these findings by showing transgene$^{+}$ Ki67$^{+}$ cells in the brain of transplanted mice both short- and long-term after HCT (Fig. 5*I*).

Interestingly, also LV integration site analysis in BU-transplanted animals indicated expansion (likely upon local proliferation) of an oligoclonal cell pool, which migrated short-term into the brain and was maintained independently from the BM HSC pool (Fig. S10 and Table S1). Of note, the TAμ cell fraction that is expanded in the transplanted mice is reminiscent of the myeloid cells found in the immature mouse brain (Fig. S11). Thus, it might represent an immature population, which could give rise in the long-term to mature microglia.

## Discussion

A critical need exists to enhance and accelerate microglia turnover with donor cells after HCT to anticipate the time of clinical benefit and improve the efficacy of the transplant in severe diseases like LSDs. For these disorders, reconstitution of microglia with donor-derived elements is of particular value being that these cells are the most abundant among the myeloid brain populations, thus the most valuable source for CNS metabolic correction. However, obtaining microglia reconstitution by the donor is a challenging goal, particularly when clinically predictive settings

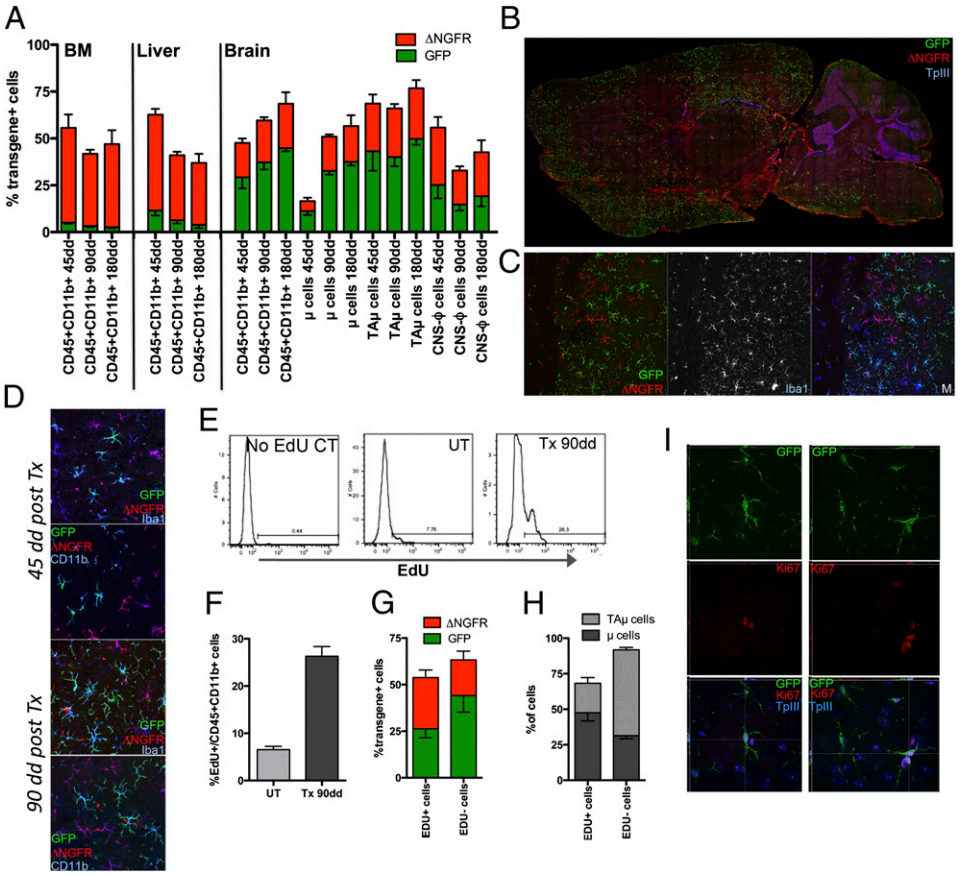


**Fig. 5.** Depletion of endogenous microglia and proliferation of donor cells in the brain for microglia reconstitution. (*A*) Frequency of transgene$^+$ [GFP (green) and ΔNGFR (red)] cells within BM and liver CD45$^+$CD11b$^+$ cells and the indicated brain populations at 45, 90, and 180 d after second HCT. (*B*) Distribution of GFP$^+$ and ΔNGFR$^+$ cells in the mouse brain at 45 d after the second HCT. GFP (green) and ΔNGFR (red) IF, and TPIII for nuclei, are shown. (*C* and *D*) Representative pictures showing transgene$^+$ cells in the mouse brain at 45 (*D*, *Upper*) and 90 (*C* and *D*, *Lower*) d after second HCT, stained for GFP (green), ΔNGFR (red), CD11b, and Iba-1. (*E*) Representative plots showing Edu$^+$ cells within CD45$^+$CD11b$^+$ cells at 90 d after the second HCT. No Edu CT, negative control of Edu staining; UT, Edu-treated age matched nontransplanted mouse. (*F*) Frequency of Edu$^+$ cells within CD45$^+$CD11b$^+$ cells in the brain of age-matched UT mice and of transplanted mice at 90 d after second HCT. (*G* and *H*) Percentage of transgene$^+$ cells (*G*) and of μ and TAμ cells (*H*) within Edu$^{+/-}$CD45$^+$CD11b$^+$ cells of the mice shown in *G*. Mean and SEM are shown and $n = 6$ mice per group for each time point in *A* and *F*–*H* (*I*) Representative pictures showing Ki67$^+$ (red) GFP$^+$ cells in the brain of BU-treated mice at 90 d after second HCT (Perkin-Elmer Confocal UltraVIEW Ers Spinning Disk Confocal, acquisition of z-stacks, processed with Volocity software) (Magnification: *C*, 20×; *D*, 50×; *I*, 63×.)

are used (9). Moreover, very little is known on the modalities of microglia turnover in physiological and pathological conditions, which may help in adequately designing therapeutic approaches.

The work here presented identifies critical factors, which could be exploited to induce successful microglia reconstitution. Indeed, by challenging different conditioning protocols in mice, we showed that only the use of a regimen, such as busulfan, capable of depleting endogeous microglia, likely through short-term killing of functionally defined precursors, allowed obtaining an efficient turnover of these cells with donor-derived elements. Importantly, the extent of long-term depletion of mature microglia correlated well with the extent of donor chimerism within the same population. Of note, the LSD microglia, which is known to be a site of storage and a critical player in disease neuropathology, is particularly sensitive to this toxic effect, thus providing a direct explanation of the higher donor chimerism observed in LSD models after HCT (Fig. S12) (7, 22). Interestingly, this concept applies also when a challenging transplant setting is used, such as the sequential transplant protocol here described. In this setting, we could rather strengthen our findings, because the ablative effect exerted by busulfan in the first HCT was strong enough to allow microglia reconstitution also by the cells transplanted after treosulfan. The latter, when used as a single agent, was not capable of inducing microglia replacement. Thus, busulfan was capable of modulating the local brain environment in a favorable manner, likely by creating "space" for the engraftment of ΔNGFR$^+$ cells. These findings suggest a unique paradigm in the brain that mimics the concept of myeloablation in the hematopoietic system at the basis of HCT practice—and of its success—for decades. Moreover, they provide hints on the mechanism of microglia maintenance during adulthood upon indirect identification of myeloid cells, which could contain bona fide microglia progenitors, whose ablation results in long-term depletion and senescence of mature microglia.

The double-transplant experiment also allowed obtaining relevant information on the mechanisms of microglia reconstitution: a sustained GFP chimerism was observed in brain myeloid cells, including antigenically and morphologically defined microglia, long-term after HCT even when a very low GFP chimerism was present in BM, peripheral blood, and other tissue macrophages. This finding, together with the identification of donor-derived cells proliferating in the brain long-term after HCT and with the appearance after HCT of progressively more mature donor cells resembling those found during postnatal development (19), suggest that microglia reconstitution can occur independently from donor engraftment in the BM and recruitment of circulating mature myeloid cells. It could result rather from expansion and maturation of donor-derived precursor cells capable of local proliferation once migrated in the brain short-term after HCT. Of note, the composition of the brain donor-derived cells in the short-term was oligoclonal compared with the BM Lin$^-$ and spleen Gr1$^+$ populations and appeared poorly developmentally related to the latter two cell populations.

Interestingly, these findings are in agreement with the recently reported observation that HSCs must be transplanted to obtain microglia turnover with the donor (23) and provide an unexpected mechanistic explanation to this latter observation. Indeed, according to our data, HSCs might be required for obtaining microglia replacement by the donor because they comprise a cell subpopulation able to replace the intraparenchymal microglia precursors that are eliminated upon myeloablative conditioning, rather than because they ensure long-term hematopoietic donor engraftment in the BM. Chemokine receptor 2 (CCR2), which was shown to play a role in microglia reconstitution (9) and to be expressed also in immature hematopoietic subsets such as myeloid progenitors (24), could be involved in the migration of BM-derived microglia progenitors into the busulfan-conditioned brain, in which the expression of CCR2 ligands is induced (Fig. S8).

This model raises issues that should be addressed in the future. First, a detailed characterization of the cells, which undergo apoptosis short-term after conditioning, is needed. Indeed, these cells may represent or comprise the long-sought, bona fide microglia progenitors, which have been described to migrate into the brain in embryonic life and to maintain the microglia pool during adulthood (2, 8). Second, the identification of the fraction within KSL cells capable of short-term brain homing and local proliferation would be of great value. Furthermore, a better characterization of the fate of donor-derived cells into the CNS would be of interest, like in the case of TAμ cells, which could represent an immature/transient population that may in the long-term replenish the mature microglia pool. Finally, the findings reported in the sequential transplant setting propose a very provocative scenario in which engraftment in hematopoietic organs might not be necessary for obtaining efficient microglia reconstitution by the donor after HCT. This scenario is consistent with the results obtained in adrenoleukodystrophy (ALD) patients treated by HSC gene therapy (25). Interestingly, in these patients, clinical benefit, comparable to that described in ALD subjects showing full donor chimerism after allogeneic HCT, was observed despite a bone marrow engraftment of the genetically corrected cells less than 15%. These patients received a busulfan-based conditioning, which could have favored a sustained brain chimerism of the transduced cells, potentially higher than the one detected in the hematopoietic system.

In conclusion, we demonstrate that a short-term wave of brain infiltration by a fraction of the transplanted hematopoietic progenitors occurs upon HCT, independently from the administration of a preparatory regimen and from the presence of a disease state in the brain; the use of a conditioning regimen capable of exerting an ablative effect on functionally defined CNS-resident myeloid precursors favors turnover of microglia with the donor cells, likely mediated by local proliferation of early immigrants. Most importantly, this work has high clinical relevance because it provides valuable suggestions for the design of alternative protocols for patients undergoing HCT or HSC gene therapy in the presence of neurological disorders requiring microglia replacement for therapeutic efficacy, as in the case of LSDs.

## Materials and Methods

**Mice Studies.** Studies were performed on $As2^{+/+}$ and $As2^{-/-}$ mice (26), maintained in the animal facility of Ospedale San Raffaele. Procedures were approved by the San Raffaele Institutional Animal Care and Use Committee (IACUC 325/439) and communicated to the Ministry of Health and local authorities.

**HSPC Transplantation.** HSPCs were purified and transduced by using two Lentiviral Vectors (LVs), pCCLsin.cPPT.humanPGK.GreenFluorescentProtein.Wpre (GFP-LV) or pCCLsin.cPPT.humanPGK.DeletedNerveGrowthFactorReceptor.Wpre (ΔNGFR-LV) (27), as described (28). Transduced HSPC transplantation was performed i.v. in 2-mo-old naïve or pretreated mice, having received different myeloablative regimens at their maximum tolerated dose, namely lethal irradiation (11 Gy administered 24 h before HCT) or the alkylating agents busulfan (C6H1406S2, Sigma; injected intraperitoneally (i.p.) 25 mg/kg from day −4 to day −1) and treosulfan (Medac; administered i.p. 7,000 mg/kg, six doses over 3 d).

**Flow-Cytometric Analysis.** Cells from BM, brain, and liver were analyzed by flow cytometry upon resuspension in blocking solution (PBS; 5% FBS and 1% BSA) and labeling at 4 °C for 15 min with: rat PE anti-mouse CD45 (BD Pharmingen) 1:100; rat Pacific Blue anti-mouse CD45.2 (Bio Legend) 1:100; rat APC anti-mouse CD11b (eBioscience) 1:100; mouse PE anti-mouse I-A/I-E (MHC class II) (BD Pharmingen) 1:250; mouse Alexa-Fluor 647 anti-Human CD271 (NGF receptor) (BD Pharmingen) 1:30; rat APC 780 anti-mouse CD11b (eBioscience) 1:100; and goat GFP antibody FITC (Abcam) 1:100.

**Statistical Analyses.** Statistical analyses were made by one-way ANOVA for repeated measurements using Bonferroni's or Dunnet's tests for post hoc analysis and by unpaired Student's *t* test (confidence interval 95%).

Please refer to *SI Materials and Methods*.

**ACKNOWLEDGMENTS.** We thank F. Pucci for isolation of inflammatory monocytes and gene expression studies, F. Benedicenti for PCR studies, A. Giustacchini for Edu staining, A. Iadanza for technical help for MR studies, G. Zanetti for assistance in bioinformatics, C. Covino for assistance in confocal image acquisition, Fabio Ciceri for fruitful discussion, and Joachim Baumgart for providing reagents. This work was supported by Italian Telethon Foundation TGT-B1, the Seventh Framework Programme (FP7)-HEALTH-2009 Program (Therapeutic Challenge in Leukodystrophies, LeukoTreat), and the Italian Ministry of Health (Progetto Giovani Ricercatori) (to A.B.).

1. Vilhardt F (2005) Microglia: Phagocyte and glia cell. *Int J Biochem Cell Biol* 37:17–21.
2. Ginhoux F, et al. (2010) Fate mapping analysis reveals that adult microglia derive from primitive macrophages. *Science* 330:841–845.
3. Ponomarev ED, Shriver LP, Maresz K, Dittel BN (2005) Microglial cell activation and proliferation precedes the onset of CNS autoimmunity. *J Neurosci Res* 81:374–389.
4. Boucsein C, et al. (2003) Purinergic receptors on microglial cells: Functional expression in acute brain slices and modulation of microglial activation in vitro. *Eur J Neurosci* 17: 2267–2276.
5. Simard AR, Rivest S (2004) Bone marrow stem cells have the ability to populate the entire central nervous system into fully differentiated parenchymal microglia. *FASEB J* 18:998–1000.
6. Priller J, et al. (2001) Targeting gene-modified hematopoietic cells to the central nervous system: Use of green fluorescent protein uncovers microglial engraftment. *Nat Med* 7:1356–1361.
7. Biffi A, et al. (2004) Correction of metachromatic leukodystrophy in the mouse model by transplantation of genetically modified hematopoietic stem cells. *J Clin Invest* 113: 1118–1129.
8. Ajami B, Bennett JL, Krieger C, Tetzlaff W, Rossi FMV (2007) Local self-renewal can sustain CNS microglia maintenance and function throughout adult life. *Nat Neurosci* 10:1538–1543.
9. Mildner A, et al. (2007) Microglia in the adult brain arise from Ly-6ChiCCR2+ monocytes only under defined host conditions. *Nat Neurosci* 10:1544–1553.
10. Peters C, Steward CG; National Marrow Donor Program; International Bone Marrow Transplant Registry; Working Party on Inborn Errors, European Bone Marrow Transplant Group (2003) Hematopoietic cell transplantation for inherited metabolic diseases: An overview of outcomes and practice guidelines. *Bone Marrow Transplant* 31: 229–239.
11. Staba SL, et al. (2004) Cord-blood transplants from unrelated donors in patients with Hurler's syndrome. *N Engl J Med* 350:1960–1969.
12. Escolar ML, et al. (2005) Transplantation of umbilical-cord blood in babies with infantile Krabbe's disease. *N Engl J Med* 352:2069–2081.
13. Krivit W, Sung JH, Shapiro EG, Lockman LA (1995) Microglia: The effector cell for reconstitution of the central nervous system following bone marrow transplantation for lysosomal and peroxisomal storage diseases. *Cell Transplant* 4:385–392.
14. Niemeyer M, et al. (2010) Non-invasive tracking of human haemopoietic CD34(+) stem cells in vivo in immunodeficient mice by using magnetic resonance imaging. *Eur Radiol* 20:2184–2193.
15. Politi LS, et al. (2007) Magnetic-resonance-based tracking and quantification of intravenously injected neural stem cell accumulation in the brains of mice with experimental multiple sclerosis. *Stem Cells* 25:2583–2592.
16. Yaghootfam A, Gieselmann V, Eckhardt M (2005) Delay of myelin formation in arylsulphatase A-deficient mice. *Eur J Neurosci* 21:711–720.
17. Westerhof GR, et al. (2000) Comparison of different busulfan analogues for depletion of hematopoietic stem cells and promotion of donor-type chimerism in murine bone marrow transplant recipients. *Cancer Res* 60:5470–5478.
18. Ford AL, Goodsall AL, Hickey WF, Sedgwick JD (1995) Normal adult ramified microglia separated from other central nervous system macrophages by flow cytometric sorting. Phenotypic differences defined and direct ex vivo antigen presentation to myelin basic protein-reactive CD4+ T cells compared. *J Immunol* 154:4309–4321.
19. Hristova M, et al. (2010) Activation and deactivation of periventricular white matter phagocytes during postnatal mouse development. *Glia* 58:11–28.
20. Streit WJ, Xue QS (2009) Life and death of microglia. *J Neuroimmune Pharmacol* 4: 371–379.
21. Kraft AD, McPherson CA, Harry GJ (2009) Heterogeneity of microglia and TNF signaling as determinants for neuronal death or survival. *Neurotoxicology* 30:785–793.
22. Sano R, Tessitore A, Ingrassia A, d'Azzo A (2005) Chemokine-induced recruitment of genetically modified bone marrow cells into the CNS of GM1-gangliosidosis mice corrects neuronal pathology. *Blood* 106:2259–2268.
23. Ajami B, Bennett JL, Krieger C, McNagny KM, Rossi FM (2011) Infiltrating monocytes trigger EAE progression, but do not contribute to the resident microglia pool. *Nat Neurosci* 14:1142–1149.
24. Schulz C, et al. (2012) A lineage of myeloid cells independent of Myb and hematopoietic stem cells. *Science* 336:86–90.
25. Cartier N, et al. (2009) Hematopoietic stem cell gene therapy with a lentiviral vector in X-linked adrenoleukodystrophy. *Science* 326:818–823.
26. Hess B, et al. (1996) Phenotype of arylsulfatase A-deficient mice: Relationship to human metachromatic leukodystrophy. *Proc Natl Acad Sci USA* 93:14821–14826.
27. Dull T, et al. (1998) A third-generation lentivirus vector with a conditional packaging system. *J Virol* 72:8463–8471.
28. Biffi A, et al. (2006) Gene therapy of metachromatic leukodystrophy reverses neurological damage and deficits in mice. *J Clin Invest* 116:3070–3082.